A ^{5}e Mossbauer study of a new series of rare-earth iron nitrides: $R_2Fe_{17}N_{3-}$ delta

1991 J. Phys.: Condens. Matter 3 3983

(http://iopscience.iop.org/0953-8984/3/22/010)

J. Phys.: Condens. Matter 3 (1991) 3983–3995. Printed in the UK

A ^{57}Fe Mössbauer study of a new series of rare-earth iron nitrides: $R_2Fe_{17}N_{3-\delta}$

Bo-Ping Hu, Hong-Shuo Li, Hong Sun and J M D Coey
Department of Pure and Applied Physics, Trinity College, Dublin 2, Ireland

Received 2 October 1990, in final form 15 February 1991

Abstract. ^{57}Fe Mössbauer spectra have been obtained at room temperature and at 15 K for R_2Fe_{17} and $R_2Fe_{17}N_{3-\delta}$ ($\delta \simeq 0.4$) with R ≡ Ce, Pr, Nd, Sm, Gd, Tb, Dy, Ho, Er, Tm, Lu and Y. The easy direction of magnetization of the R_2Fe_{17} compounds can be identified by analysis of the hyperfine field and quadrupole interactions. For rare-earth elements with $J > 3$, the sixth-order crystal-field parameter B_{66} determines the easy magnetization direction in the basal plane. In the nitrides, the average hyperfine field at 15 K increases by approximately 13% above the value in the parent compounds, from about 31 to 35 T, and it is anisotropic, being greatest when the magnetization lies along the *c*-axis. There is also an increase in the isomer shift of 0.12(2) mm s^{-1}. Spin reorientation transitions occur in the nitrides of Er and Tm; only the samarium nitride has an easy *c*-axis at room temperature, but Sm, Er and Tm all have easy *c*-axis magnetic structures at 15 K.

1. Introduction

Recent interest in rare-earth iron magnetic materials has shifted to the novel ternary nitrides $R_2Fe_{17}N_{3-\delta}$ [1–5]. It is known that the magnetic properties of R_2Fe_{17} intermetallics can be improved by the interstitial atoms H [6–9] and C [10, 11], which raise the Curie temperature T_C by up to 200 K. The effect of nitrogen on T_C is even greater, producing increases of about 400 K. At room temperature, the $R_2Fe_{17}X_y$ compounds (X ≡ H, C and N) usually have the same easy direction, with the magnetization lying in the basal plane as it does in R_2Fe_{17}. The exceptions are the $Sm_2Fe_{17}X_{3-\delta}$ (X ≡ C and N; $\delta \leq 2.5$). $Sm_2Fe_{17}C$ shows a uniaxial anisotropy field of 5.3 T at room temperature [12, 19], whereas the room temperature anisotropy field of $Sm_2Fe_{17}N_2$ has been found to be 14 T [3]. The combination of high Curie temperature of 749 K [2], high saturation polarization of about 1.5 T [1,3] and strong uniaxial anisotropy make $Sm_2Fe_{17}N_{3-\delta}$ a most promising material for permanent magnets.

The iron-rich R_2Fe_{17} compounds have been studied for many years [13, 14]. They exist across the whole lanthanide series, except for La itself, crystallizing in the rhombohedral Th_2Zn_{17} structure for rare earths lighter than Gd, and in the hexagonal Th_2Ni_{17} structure for rare earths heavier than Tb; both structure types may coexist for R ≡ Gd, Tb and Y [14]. In this paper, the site notation is given first for the hexagonal structure, with the notation for the corresponding sites for the rhombohedral structure in brackets (e.g. $4f(6c)$ for the dumbell site). The magnetic structure is governed by the predominantly ferromagnetic Fe–Fe coupling, the R–Fe exchange which tends to align rare-earth and iron spins antiparallel, the rare-earth crystal-field

interactions and Fe sublattice anisotropy. At low temperature the easy magnetization direction in R_2Fe_{17} coincides with one of the main axes of the basal plane [15], except for Tm_2Fe_{17} which has an easy c-axis [16,17], and Ce_2Fe_{17} [18], Yb_2Fe_{17} [20] and Lu_2Fe_{17} [18] which all have canted or helical structures.

^{57}Fe Mössbauer investigations of R_2Fe_{17} have been performed by Gubbens and others [8, 16, 21–25]. Because of the complex crystal structure, only an average hyperfine field [21] or the distinctly separate contribution of the $4f(6c)$ dumbell site was determined [22] in the early studies. Gubbens, however, used six independent iron subspectra to analyse the spectra of R_2Fe_{17}. There is one subspectrum for each of the $4f(6c)$ and $6g(9d)$ sites, but the $12j(18f)$ and $12k(18h)$ sites split into two groups in a 2:1 ratio due to the different angles between the magnetization direction and the principal axis of the electric field gradient [23]. Tm_2Fe_{17} is an exception below its spin reorientation at 72 K [16, 17]; four subspectra suffice when the magnetization lies parallel to c-axis. A further complication is caused by the magnetic dipolar field when the magnetization is along the a-axis ([100]) or the b-axis ([120]). The observed hyperfine field is the sum of an atomic contribution and a dipolar contribution due to the moments of all the other atoms. The resulting sum of these contributions need not have a single value at particular crystallographic sites. In fact seven or eight subspectra are necessary to analyse the Mössbauer data on compounds with the Th_2Zn_{17} or Th_2Ni_{17} structures respectively [24].

Structural considerations indicate that the only interstitial sites large enough to accommodate nitrogen atoms in $R_2Fe_{17}N_{3-\delta}$ are $6h(9e)$ [5]. The same is true for interstitial carbon atoms in $R_2Mn_{17}C_{3-\delta}$ [26]. This has been confirmed by EXAFS for $Sm_2Fe_{17}N_{2.3}$ [5], by neutron diffraction for $Nd_2Fe_{17}N_{3-\delta}$ [27] and by x-ray diffraction for $R_2Fe_{17}C_{3-\delta}$ [28]. The crystal structures of rhombohedral and hexagonal $R_2Fe_{17}N_3$ are shown in figure 1.

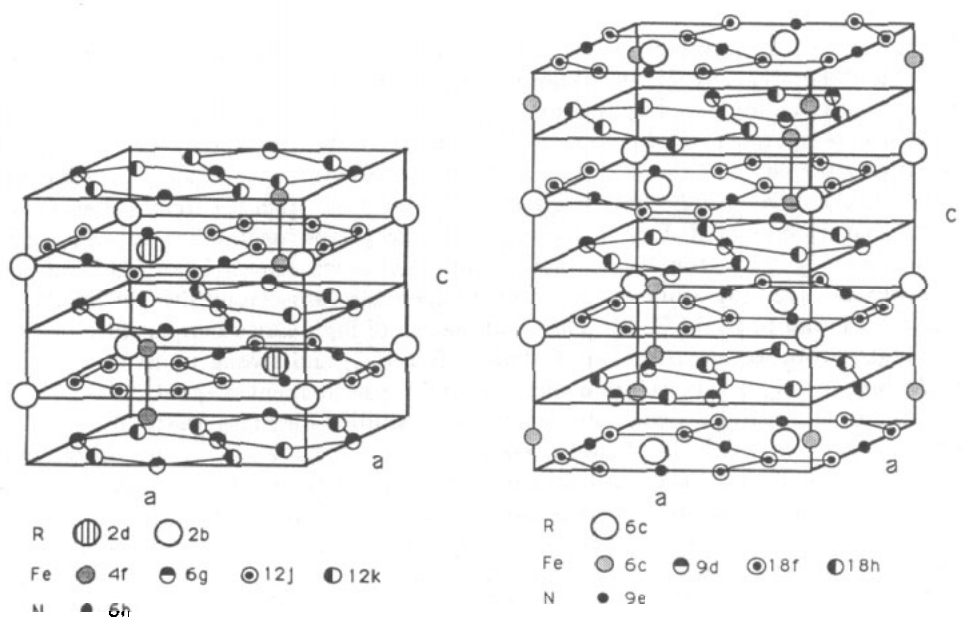

Figure 1. Crystal structures of the hexagonal (left) and rhombohedral (right) varieties of $R_2Fe_{17}N_3$.

In this work, ^{57}Fe Mössbauer effect measurements have been performed at 15 K and room temperature on a series of R_2Fe_{17} compounds and on the corresponding $R_2Fe_{17}N_{3-\delta}$ nitrides, with a view to developing an understanding of the magnetic properties of the nitrides on the atomic scale.

2. Experimental methods

The R_2Fe_{17} compounds were prepared by arc-melting 99.9% pure elements and annealing the ingots of the lighter rare earth compounds up to Gd in vacuum at 1000 °C for about 50 h. Analysis by x-ray diffraction showed that the compounds of rare earths lighter than Tb have the rhombohedral Th_2Zn_{17} structure whereas the others have the hexagonal Th_2Ni_{17} structure. X-ray patterns also showed some traces of α-Fe in the Nd and Sm compounds.

The nitrogen absorption characteristic was then observed for each compound by heating a small amount of fine powder ($\sim$ 50 mg) at 10 °C min^{-1} in approximately 1 bar of N_2 gas in a thermopiezic analyser [29]. A suitable temperature for nitrogenation was determined, which is always in the range of 450 to 550 °C. The nitrogen concentration in the alloy was deduced from the pressure drop observed on cycling up to the maximum temperature T_m and back to room temperature. X-ray patterns showed that some poorly crystallized α-Fe is present in all the nitrides.

^{57}Fe Mössbauer spectra were collected using a conventional constant acceleration spectrometer with a 20 mCi source of ^{57}Co in rhodium. The velocity scale was calibrated using an α-Fe absorber at room temperature. Samples consisted of about 15 mg cm^{-2} of $R_2Fe_{17}N_{3-\delta}$ powder mixed with icing sugar to form homogeneous and isotropic absorbers. Low temperature data were obtained using a closed-cycle two-stage helium refrigerator (Air Products Model, HC-2).

3. Experimental results and analysis

In order to determine the number of subspectra employed in the fit, dipole fields were estimated for the whole R_2Fe_{17} series by summing the contributions of atoms within a 1.0 nm sphere. (We are only concerned here with the local symmetry of the dipole field rather than its magnitude.) Regardless of whether the magnetization lies along the *a* or *b*-axis, all the Fe sites (except the dumbell sites) split into several groups with different dipolar fields. When the magnetization lies along the *c*-axis ([001]), the dipolar field at each type of site has a common magnitude. In the Th_2Zn_{17}-type structure, 9*d*, 18*h* and 18*f* each split into two groups with an intensity ratio 2:1, while in the Th_2Ni_{17}-type structure 6*g* and 12*k* split into two groups with an intensity ratio 2:1, and 12*j* splits into three groups with an intensity ratio 1:1:1. This result agrees with a similar calculation for Y_2Fe_{17} [24].

Under the combined effects of the hyperfine fields (including dipolar fields) and quadrupole interactions, each of the seven or eight sextets exhibits specific values for the magnetic hyperfine interaction and quadrupole splitting. Since the dipolar fields at two of the three groups of 12*j* sites in the Th_2Ni_{17}-type compounds are very close, we treat them in the same way as for the 18*f* sites in the Th_2Zn_{17}-type compounds, splitting them into two groups with an intensity ratio 2:1. Hence the spectra of all the R_2Fe_{17} compounds were fitted to the seven independent Lorentzian sextets by

least-squares computer minimization, with an overall intensity ratio of 1:2:2:4:2:4:2 for the $6g_1(9d_1)$, $6g_2(9d_2)$, $12j_1(18f_1)$, $12j_2(18f_2)$, $12k_1(18h_1)$, $12k_2(18h_2)$ and $4f(6c)$ subspectra. The spectra of R_2Fe_{17} together with the envelope of the fits are shown in figure 2 (at 15 K) and figure 3 (at 293 K). Different linewidths were permitted for outer, middle and inner pairs of lines ($\Gamma_{3,4} < \Gamma_{2,5} < \Gamma_{1,6}$), but these linewidths were all in the range 0.28–0.36 mm s^{-1} full width at half maximum.

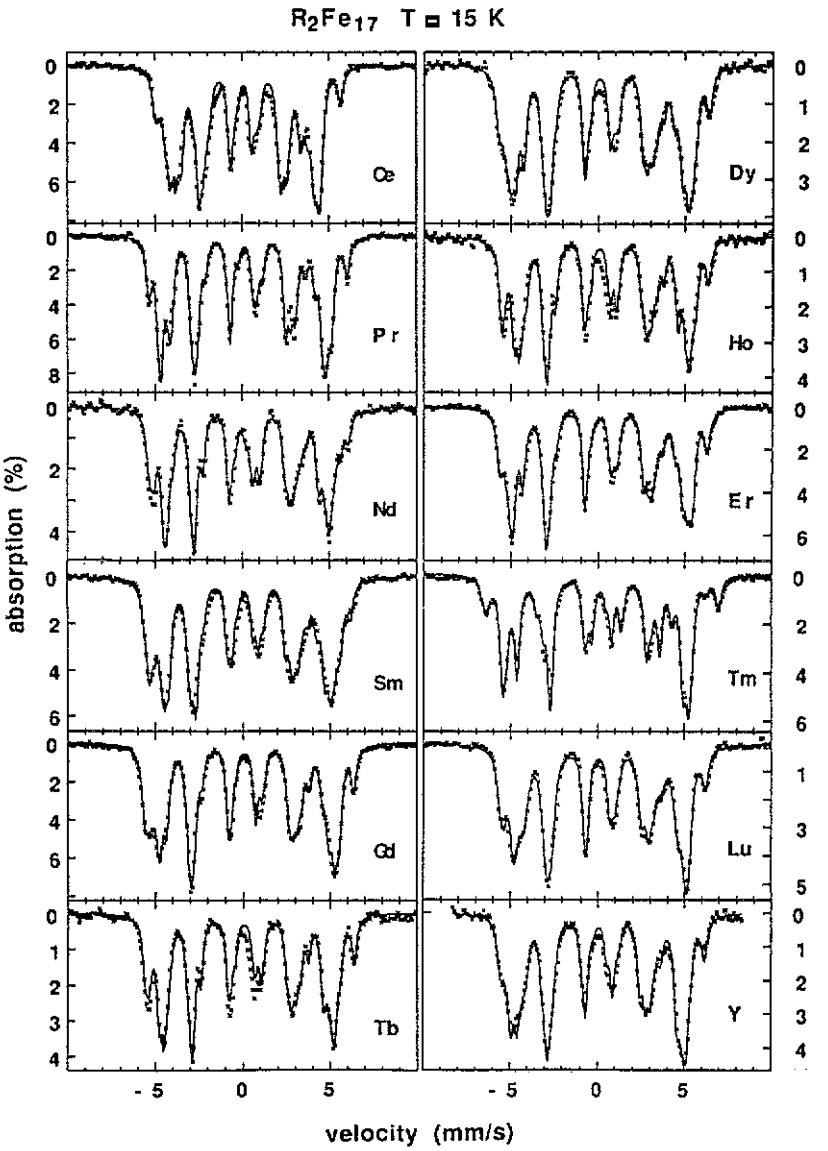

Figure 2. The ^{57}Fe Mössbauer spectra of R_2Fe_{17} at 15 K with the fits shown as full curves.

For the nitrides of the 2:17 compounds, the pressure drop in the thermopiezic analyser indicates that there are fewer than three nitrogen atoms in a 2:17 formula.

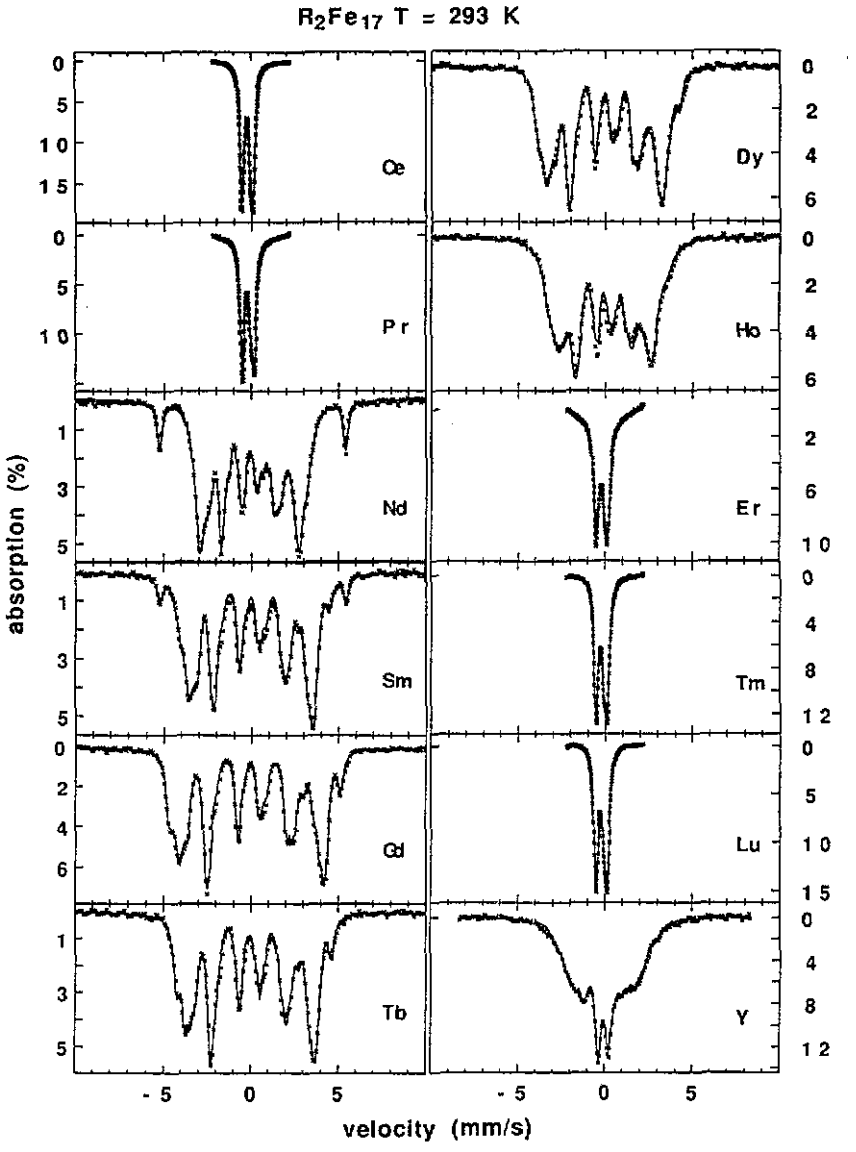

Figure 3. The ^{57}Fe Mössbauer spectra of R_2Fe_{17} at 293 K with the fits shown as full curves.

The $12j(18f)$ and $12k(18h)$ iron sites have one neighbouring octahedral interstitial site, hence they can have only one or no nitrogen neighbours. The probability for one neighbour in $R_2Fe_{17}N_{3-\delta}$ is much larger than that for no neighbours when δ is close to 0. For example, if $\delta = 0.5$, these probabilities are 0.83 and 0.17, respectively. Hence, it is reasonable to fit the Mössbauer spectra of $R_2Fe_{17}N_{3-\delta}$ using the same procedure as for R_2Fe_{17}, and to ignore the small effect of zero nitrogen nearest neighbours on the $12j(18f)$ and $12k(18h)$ sites. The Mössbauer spectra of $R_2Fe_{17}N_{3-\delta}$, together with their envelope of the fits are shown in figure 4 (at 15 K) and figure 5 (at 293 K).

During the fitting, a small α-Fe spectrum was included for Nd_2Fe_{17} and Sm_2Fe_{17}

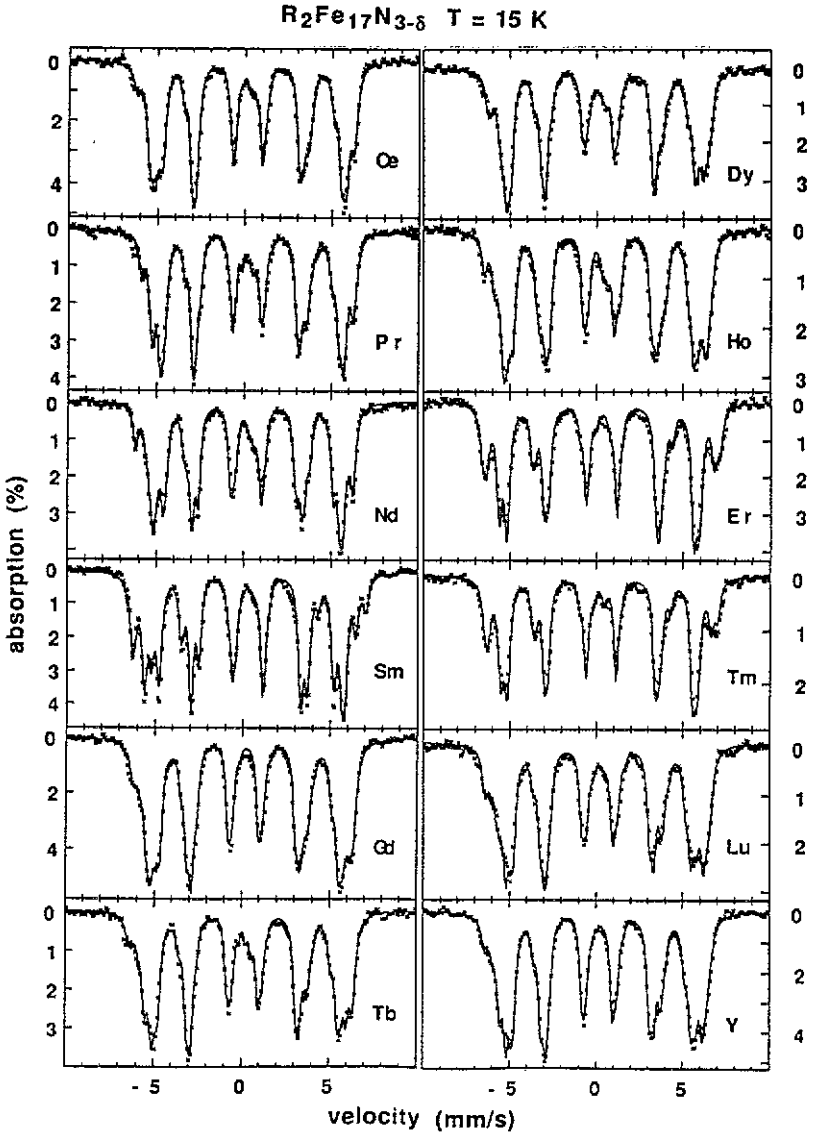

Figure 4. The ^{57}Fe Mössbauer spectra of $R_2Fe_{17}N_{3-\delta}$ at 15 K with the fits shown as full curves.

and for all the nitrides. The parent compounds of the light rare earths do not melt congruently, and further α-Fe is usually produced during nitrogenation. In addition, a weak central paramagnetic doublet of uncertain origin (< 3% of total absorption) was introduced for some of the spectra. The hyperfine fields at the four crystallographic sites of R_2Fe_{17} and $R_2Fe_{17}N_{3-\delta}$ are listed in tables 1 and 2, respectively; where two or three subspectra arise from a particular crystallographic site, the weighted average has been taken. The overall average hyperfine fields are plotted in figure 6. No values are shown for parent compounds at room temperature for R < Nd and R > Ho since their Curie temperatures are less than (or in the case of Er_2Fe_{17} practically equal to) the measuring temperature [2].

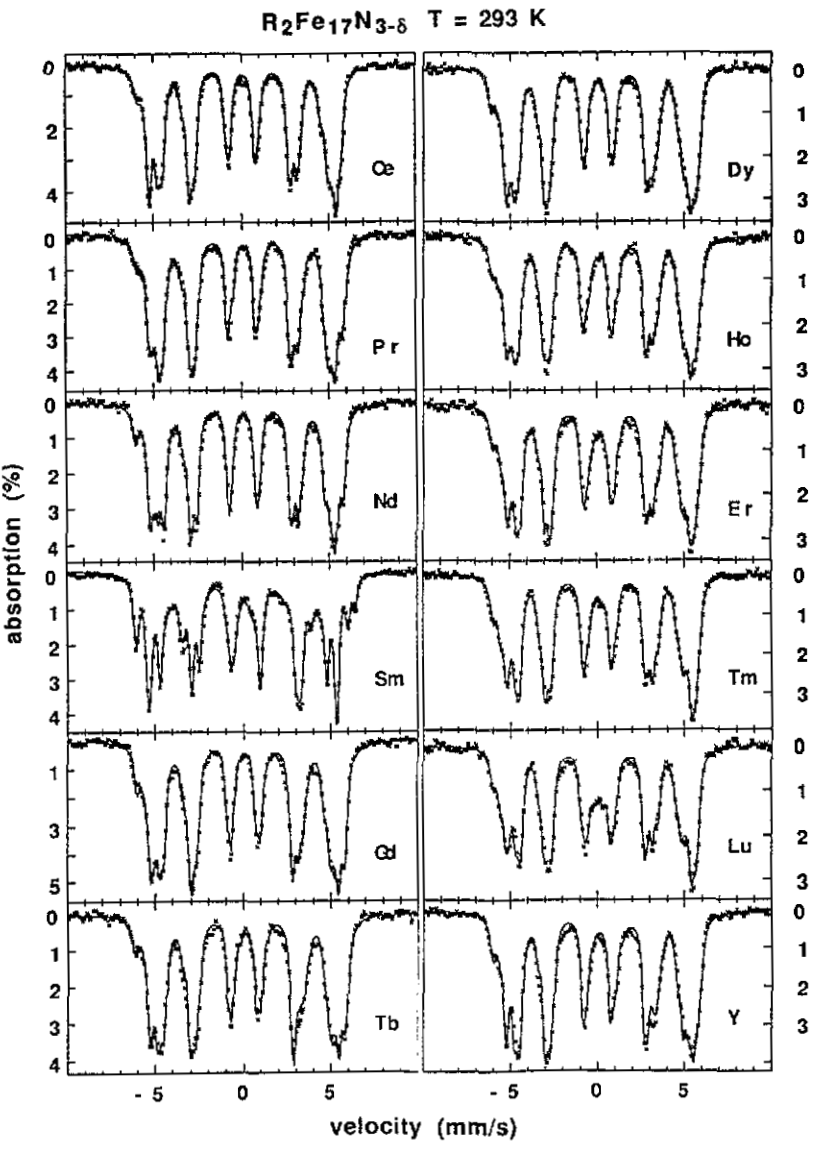

Figure 5. The ^{57}Fe Mössbauer spectra of $R_2Fe_{17}N_{3-\delta}$ at 293 K with the fits shown as full curves.

4. Discussion

To assign the components of the spectra to the iron sites, we had to consider nearest-neighbour environments, using the same arguments as for the $R(Fe_{11}Ti)$ series [30]. The number of nearest-neighbour atoms for $4f(6c)$, $6g(9d)$, $12j(18f)$ and $12k(18h)$ sites are (1, 3, 6, 3, 1), (2, 0, 4, 4, 2), (2, 2, 2, 4, 2) and (1, 2, 4, 2, 3) respectively, where the numbers in brackets refer to $4f(6c)$, $6g(9d)$, $12j(18f)$ and $12k(18h)$ and $2b$, $2d(6c)$ site neighbours. There is no doubt that the $4f(6c)$ dumbell site should have the largest hyperfine field since it has the most iron, and the fewest rare-earth neighbours. Similarly, the $12j(18f)$ site has a larger hyperfine field than the $12k(18h)$

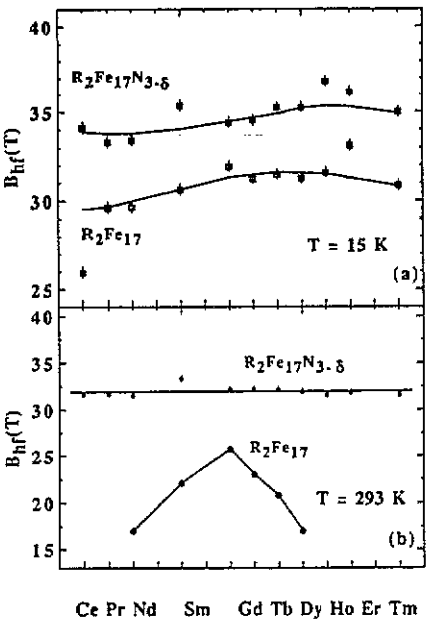

Figure 6. Overall average hyperfine fields for R_2Fe_{17} and of $R_2Fe_{17}N_{3-\delta}$ compounds: (*a*) at 15 and (*b*) at 293 K.

Table 1. Hyperfine fields for each crystallographic site of the R_2Fe_{17} deduced from ^{57}Fe Mössbauer spectra (averaging over subspectra where appropriate), and the overall average value: (*a*) at 15 and (*b*) at 293 K. In the last column of (*a*), the values of x are given, where x is defined as in the formula $R_{2-x}Fe_{17+2x}$.

R	6*g*(9*d*) (T)	12*k*(18*h*) (T)	12*j*(18*f*) (T)	4*f*(6c) (T)	$\langle B_{hf}\rangle$ (T)	x
(*a*)						
Ce	27.7(5)	23.6(3)	25.5(5)	33.1(2)	25.9(3)	−0.17(6)
Pr	31.6	27.2	29.2	35.5	29.6	−0.03
Nd	32.0	27.5	28.9	35.8	29.7	−0.13
Sm	34.0	28.1	30.0	35.9	30.7	−0.14
Gd	34.0	29.1	31.8	37.2	32.0	0.20
Tb	33.8	29.1	29.9	37.2	31.3	0.11
Dy	33.4	28.5	31.5	37.5	31.5	0.06
Ho	34.2	29.1	30.0	36.9	31.3	0.09
Er	33.4	28.7	31.5	37.0	31.6	0.16
Tm	33.6	29.7	33.0	41.6	33.1	0.15
Lu	32.8	28.0	30.5	36.7	30.9	0.17
Y	32.5	28.2	30.6	36.5	30.8	0.00
(*b*)						
Nd	17.8(5)	16.1(3)	16.5(5)	20.9(2)	17.1(3)	
Sm	23.4	20.3	22.1	26.5	22.1	
Gd	26.1	23.5	26.1	30.5	25.8	
Tb	23.9	21.1	22.7	27.7	23.0	
Dy	21.8	19.5	20.2	25.5	20.8	
Ho	17.5	15.7	16.8	21.5	17.1	
Y	—	—	—	—	9.4	

Table 2. Hyperfine fields for each crystallographic site of the $R_2Fe_{17}N_{3-\delta}$ deduced from ^{57}Fe Mössbauer spectra (averaging over subspectra where appropriate) and the overall average value: (*a*) at 15 K and (*b*) at 293 K.

R	$6g(9d)$ (T)	$12k(18h)$ (T)	$12j(18f)$ (T)	$4f(6c)$ (T)	$\langle B_{hf} \rangle$ (T)
(*a*)					
Ce	36.7(5)	31.4(3)	34.2(5)	38.3(2)	34.1(3)
Pr	35.6	30.8	33.3	37.7	33.3
Nd	36.1	30.5	33.3	38.8	33.5
Sm	39.4	31.1	35.6	41.6	35.4
Gd	36.7	31.5	34.8	38.8	34.5
Tb	37.2	31.6	34.6	39.5	34.6
Dy	37.3	32.6	35.3	40.1	35.3
Ho	36.8	32.3	35.8	40.7	35.3
Er	40.7	33.5	35.9	42.5	36.8
Tm	39.9	33.1	35.3	41.7	36.2
Lu	37.1	31.7	35.5	40.4	35.0
Y	36.8	31.6	35.2	40.2	34.8
(*b*)					
Ce	33.6(5)	28.9(3)	31.9(5)	35.9(2)	31.6(3)
Pr	34.2	29.2	31.3	36.6	31.7
Nd	34.1	28.7	31.2	36.9	31.5
Sm	37.3	29.5	33.3	39.0	33.3
Gd	34.6	29.6	32.0	36.7	32.2
Tb	34.6	29.2	32.3	37.2	32.2
Dy	33.8	29.2	32.6	37.3	32.2
Ho	33.8	29.0	32.2	37.2	31.9
Er	33.5	28.5	31.9	37.0	31.6
Tm	34.5	28.7	32.0	36.5	31.8
Lu	34.2	28.4	31.9	36.6	31.6
Y	34.0	28.5	32.2	36.9	31.8

site. The $6g(9d)$ site can be distinguished by its intensity from the $12j(18f)$ and $12k(18h)$ sites. Hence we find hyperfine fields for the iron sites that decrease in the order $4f(6c) > 6g(9d) > 12j(18f) > 12k(18h)$. This attribution of hyperfine fields is consistent with neutron diffraction results on the Nd_2Fe_{17} compound [31] and band calculations on Y_2Fe_{17} [32].

From figure 6 we can see that the hyperfine field at 15 K for Tm_2Fe_{17} is higher than for any of the other compounds (especially on the dumbell site, tables 1(*a*) and 2(*a*)). This is related to the magnetization direction of Tm_2Fe_{17}, which is along the *c*-axis below 72 K [16,17], while the magnetization directions for the other compounds are in the *c*-plane. This anisotropy of hyperfine field is due to the unquenched 3d orbital moment, which was measured in Y_2Fe_{17} [25].

The subspectra for the site with the smallest hyperfine field $12k(18h)$ can be used to distinguish the easy magnetization direction in the *c*-plane. There are two subspectra: one with one-third of the intensity, $12k_1(18h_1)$, and the other with two-thirds, $12k_2(18h_2)$. In table 3, the quadrupolar splittings (QS) of these two components are listed for R_2Fe_{17} series. Negative values correspond to the small peak on the inner edge of the outer line at positive velocity (see figure 2). It can be seen that for R $\equiv$ Ce, Pr, Sm, Gd, Dy and Er the $12k_1(18h_1)$ component has a negative QS while for R $\equiv$ Nd, Tb, Ho, Lu and Y the $12k_2(18h_2)$ does. According to the single crystal

Table 3. Quadrupole splitting (in units of mm s^{-1}) for the two components arising from $12k(18h)$ sites of R_2Fe_{17} at 15 K. The $12k_1(18h_1)$ and $12k_2(18h_2)$ subspectra have an intensity ratio of 1:2. γ_J is the sixth-order Stevens coefficient of the trivalent rare earth.

R	Easy-axis	$12k_1(18h_1)$	$12k_2(18h_2)$	γ_J
Ce	*a*	−0.7(1)	0.4(1)	0
Pr	*a*	−0.7	0.3	+
Nd	*b*	0.5	−0.4	−
Sm	*b*	0.5	−0.3	0
Gd	*a*	−0.6	0.3	0
Tb	*b*	0.6	−0.4	−
Dy	*a*	−0.6	0.4	+
Ho	*b*	0.7	−0.4	−
Er	*a*	−0.6	0.3	+
Tm	*c*	0.1		−
Lu	*b*	0.6	−0.2	0
Y	*b*	0.6	−0.11	0

magnetization measurements on R_2Fe_{17} compounds [15], Dy_2Fe_{17} and Er_2Fe_{17} have an easy *a*-axis while Tb_2Fe_{17} and Ho_2Fe_{17} have an easy *b*-axis. By comparison, it can be concluded that the sign of QS of the $12k(18h)$ site components is related to the easy direction in the basal plane. Table 3 also lists the sixth-order Stevens coefficient γ_J of the R^{3+} ions; positive γ_J correlates with an easy *a*-axis whereas negative γ_J correlates with an easy *b*-axis. The only off-diagonal crystal-field term at $2b$ and $2d$ rare-earth sites in the hexagonal structure is $B_{66}O_{66}$; therefore it is the sign of the sixth-order crystal-field parameter B_{66} which influences the easy axis in the basal plane. The magnitude of the $B_{43}O_{43}$ and $B_{63}O_{63}$ terms at the 6*c* rare-earth site in the rhombohedral structure is expected to be relatively small compared with that of $B_{66}O_{66}$, because the two structures are very similar and have roughly the same planar environment for rare-earth atoms. The iron sublattices also contribute to the in-plane anisotropy, as is evident from the data in table 3 for rare earths that are either non-magnetic or have $J < 3$. It seems that the preferred direction for iron changes from *a* in the rhombohedral structure to *b* in the hexagonal structure.

At 15 K, the average hyperfine fields of $R_2Fe_{17}N_{3-\delta}$ are about 4 T higher than for the parent R_2Fe_{17} compounds. $Ce_2Fe_{17}N_{3-\delta}$ is an exception; there an increase of about 8.0 T is observed. If the usual proportionality of hyperfine field and magnetic moment can be applied [33], the increase of hyperfine field corresponds to a 13% increase in the iron moment and thus will contribute to the increase in T_C. The main reason for the increase in T_C across the series is nonetheless the change in Fe–Fe exchange related to the volume expansion of approximately 6–7% (table 4) which will cause a narrowing of the 3d-band, and a corresponding tendency to localization of the Fe moment.

There is an increase in the average ^{57}Fe isomer shift (IS) on nitrogenation of 0.12(2) mm s^{-1}. In particular, there is large (0.16(3)) increase in the isomer shift at $12j(18f)$ site where the iron is closest to the nitrogen, but the isomer shift at $4f(6c)$ dumbell sites is unchanged or decreases for most of the series. The volume expansion will also provoke a volume scaling of 4*s* conduction electron density, which is largely responsible for the volume dependence of the isomer shift. A volume coefficient $\delta IS/\delta \ln V = 1.31$ mm s^{-1} has been obtained for α-Fe [34]. Values of 1.0(2) mm s^{-1}

Table 4. Overall average isomer shift (IS) at 15 K (with respect to the IS of α-Fe) for R_2Fe_{17} and $R_2Fe_{17}N_{3-\delta}$ compounds. The volumes, the relative change in volume on nitrogenation and the volume coefficient of the isomer shift are also given.

	R_2Fe_{17} (15 K)		$R_2Fe_{17}N_{3-\delta}$ (15 K)				
R	IS (mm s^{-1})	V (nm^3)	IS (mm s^{-1})	V nm^3	δIS (mm s^{-1})	$\delta V/V$ (%)	δIS/$\delta \ln V$ (mm s^{-1})
Ce	−0.09(2)	0.255(1)	0.04(2)	0.278(1)	0.13	8.85	1.5
Pr	−0.06	0.264	0.07	0.258	0.13	6.47	2.0
Nd	−0.06	0.263	0.04	0.280	0.10	6.15	1.6
Sm	−0.07	0.262	0.04	0.278	0.11	6.27	1.8
Gd	−0.06	0.260	0.05	0.276	0.11	6.18	1.8
Tb	−0.06	0.258	0.03	0.274	0.09	6.40	1.4
Dy	−0.08	0.257	0.04	0.273	0.12	6.43	1.9
Ho	−0.06	0.255	0.06	0.272	0.12	6.48	1.8
Er	−0.09	0.254	0.04	0.271	0.13	6.85	1.9
Tm	−0.07	0.253	0.04	0.270	0.11	6.96	1.5
Lu	−0.07	0.252	0.04	0.270	0.11	7.13	1.5
Y	−0.11	0.257	0.04	0.274	0.15	6.42	2.3

are found for various close-packed matrices. The experimental value of δIS/$\delta \ln V$ on nitrogenation is in the range of 1.4–2.3 mm s^{-1}, which suggests that some interband electron transfer occurs on nitrogenation.

The Ce compound is exceptional; its volume expansion, $\delta \ln V = 9\%$, is much bigger than others, and there is a correspondingly large change in hyperfine field and Curie temperature. This may well reflect a change in the Ce valence state. In Ce_2Fe_{17}, the cerium is close to quadrivalent $4f^0$ [13] whereas in $Ce_2Fe_{17}N_{3-\delta}$ it is close to trivalent $4f^1$.

Further influences of nitrogenation on the magnetic properties are observed. At 15 K, it was found that $Sm_2Fe_{17}N_{3-\delta}$, $Er_2Fe_{17}N_{3-\delta}$ and $Tm_2Fe_{17}N_{3-\delta}$ all have an easy c-axis. By contrast, only Tm_2Fe_{17} has an easy c-axis in the parent series. This change in anisotropy is mainly due to the change of rare-earth local environment, as the magnetic measurements show that the Fe sublattice anisotropy is not much changed (remaining in the basal plane [4]). As can be seen from figure 1, for each R ion there are three nitrogen neighbours located in the same c-plane [5]. This excess basal-plane electronic charge density will enhance the magnitude of a negative second-order crystal-field coefficient A_{20} [35]. Therefore R ions with a positive second-order Stevens coefficient α_J (Sm, Er, Tm and Yb) will have uniaxial anisotropy. The competition of R and Fe anisotropy in the latter group (positive for Sm, Er, Tm and Yb, and negative for Fe) is confirmed by the observation of spin reorientation transitions for $Er_2Fe_{17}N_{3-\delta}$ at 120 K and for $Tm_2Fe_{17}N_{3-\delta}$ at 200 K [4]. At room temperature, only $Sm_2Fe_{17}N_{3-\delta}$ exhibits an easy c-axis.

The Th_2Ni_{17} and Th_2Zn_{17} structures are both derived from the $CaCu_5$-type structure in which one-third of the R atoms are substituted by pairs of transition-metal atoms (dumbells). The difference between these two structures is in the sequence of the dumbell substitution. Furthermore a random substitution gives the $TbCu_7$-type structure [36]. There is often a deviation from the ideal substitution in that the number of rare-earths substituted by transition-metal dumbells differs from exactly one-third [25]. Writing the formula more generally as $R_{2-x}T_{17+2x}$, x is found to be negative for light rare-earth compounds with the Th_2Zn_{17} structure and positive for

heavy rare-earth compounds with the Th_2Ni_{17} structure. Figure 7 shows the value of x deduced from the intensities of the $4f(6c)$ sites (which were unconstrained in the fits for this purpose), as a function of rare-earth element for the R_2Fe_{17} series. The step seen in this figure corresponds to the change in structure, except that Gd lies on the 'wrong' side. A similar feature has been discussed by Gubbens [23].

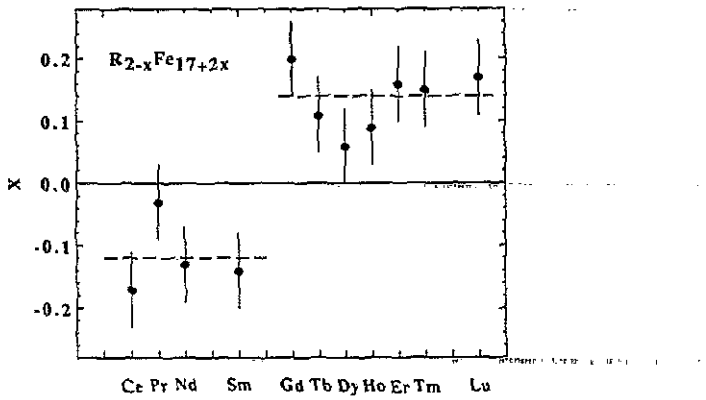

Figure 7. x as a function of rare-earth element; here x is defined as in $R_{2-x}Fe_{17+2x}$.

5. Conclusion

Systematic ^{57}Fe Mössbauer studies on R_2Fe_{17} and $R_2Fe_{17}N_{3-\delta}$ at 15 K and room temperature revealed several interesting features of the novel nitride series. The spectra are complex and the fits may not be unique in all their details, but definite conclusions can nevertheless be drawn.

The overall average hyperfine field at 15 K increases by approximately 13% in the nitrides above the value in the parent compounds. The hyperfine field in both series shows an anisotropic character, most pronounced for $4f(6c)$ and $6g(9d)$ sites. The average field at these two sites is approximately 3 T higher when the magnetization is along the c-axis. The increase in the average isomer shift is larger than expected from volume expansion, which suggests electron transfer between N 2p and Fe 3d orbitals. It is also suggested that in $Ce_2Fe_{17}N_{3-\delta}$ the Ce ion has a valence state close to 3+ whereas in Ce_2Fe_{17} it is close to 4+.

For pure R_2Fe_{17}, the easy axis can be distinguished by analysis of the hyperfine fields and quadrupole interactions. In particular, the easy magnetization direction of those compounds having easy c-plane anisotropy can be determined unambiguously by the quadrupole splitting of the $12k(18h)$ site. It was found that the easy direction in the basal plane is largely determined by the sixth-order Stevens coefficient γ_J of the rare-earth trivalent ions.

Easy c-axis anisotropy is observed for $Sm_2Fe_{17}N_{3-\delta}$, $Er_2Fe_{17}N_{3-\delta}$ and $Tm_2Fe_{17}N_{3-\delta}$ at 15 K, but it only persists at room temperature for $Sm_2Fe_{17}N_{3-\delta}$.

Acknowledgments

This work forms part of the Concerted European Action on Magnets. It was supported as part of the BRITE/EURAM programme of the European Commission.

References

[1] Coey J M D and Sun Hong 1990 *J. Magn. Magn. Mater.* **87** L251
[2] Sun Hong, Coey J M D, Otani Y and Hurley D P F 1990 *J. Phys.: Condens. Matter* **2** 6465
[3] Katter M, Wecker J, Schultz L and Grössinger R 1990 *J. Magn. Magn. Mater.* **92** L14
[4] Hu Bo-Ping, Li Hong-Shuo, Sun Hong, Lawler J F and Coey J M D 1990 *Solid State Commun.* **76** 587
[5] Coey J M D, Lawler J F, Sun Hong and Allan J E M 1991 *J. Appl. Phys.* **69** 3007
[6] Wang Xian-Zhong, Donnelly K, Coey J M D, Chevalier B, Etourneau J and Berlureau T 1988 *J. Mater. Sci.* **23** 329
[7] Hu Bo-Ping and Coey J M D 1968 *J. Less-Common Met.* **142** 295
[8] Rupp B and Wiesinger G 1988 *J. Magn. Magn. Mater.* **71** 269
[9] Rupp B, Resnik A, Shaltiel D and Rogl P 1988 *J. Mater. Sci.* **23** 2133
[10] Zhong Xia-Ping, Radwanski R J, de Boer F R, Jacobs T H and Buschow K H J 1990 *J. Magn. Magn. Mater.* **86** 333
[11] Sun Hong, Hu Bo-Ping, Li Hong-Shuo and Coey J M D 1990 *Solid State Commun.* **74** 727
[12] Kou X C, Grössinger R, Jacobs T H and Buschow K H J 1990 *J. Magn. Magn. Mater.* **88** 1
[13] Buschow K H J 1977 *Rep. Prog. Phys.* **40** 1179
[14] Wallace W E 1985 *Prog. Solid State Chem.* **16** 127
[15] Sinnema S 1988 *PhD Thesis* University of Amsterdam
[16] Gubbens P C M and Buschow K H J 1973 *J. Appl. Phys.* **44** 3739
[17] Elemans J B A A and Buschow K H J 1974 *Phys. Status Solidi* a **24** K125
[18] Givord D and Lemaire R 1974 *IEEE Trans.* **MAG-10** 109
[19] Grössinger R, Kou X C, Jacobs T H and Buschow K H J 1991 *J. Appl. Phys.* **69** in press
[20] Czjzek G, Bornemann H J, Kmiec R and Buschow K H J 1990 *J. Appl. Phys.* **67** 4625
[21] Levinson L M, Rosenberg E, Shaulov A and Strnat K 1970 *J. Appl. Phys.* **41** 910
[22] Buschow K H J and van Wieringen J S 1970 *Phys. Status Solidi* **42** 231
[23] Gubbens P C M 1977 *PhD Thesis* University of Leiden
[24] Steiner W and Haferl R 1977 *Phys. Status Solidi* a **42** 739
[25] Averbuch-Pouchot M T, Chevalier R, Déportes J, Kebe B and Lemaire R 1987 *J. Magn. Magn. Mater.* **68** 190
[26] Block G and Jeitschko W 1986 *Inorg. Chem.* **25** 279
[27] Miraglia S, Soubeyroux J L, Kolbeck C, Isnard O, Fruchart D and Guillot M 1991 *Preprint*
[28] de Mooij D B and Buschow K H J 1988 *J. Less-Common Met.* **142** 349
[29] Ryan D H and Coey J M D 1986 *J. Phys. E: Sci. Instrum.* **19** 693
[30] Hu Bo-Ping, Li Hong-Shuo and Coey J M D 1989 *Hyperfine Interact.* **45** 233
[31] Herbst J F, Croat J J, Lee R W and Yelon W B 1982 *J. Appl. Phys.* **53** 250
[32] Szpunar B and Szpunar J A 1985 *J. Appl. Phys.* **57** 4130
[33] Gubbens P C M, van Apeldoorn J H F, van der Kraan A M and Buschow K H J 1974 *J. Phys. F: Met. Phys.* **4** 921
[34] Williamson D L 1978 *Mössbauer Isomer Shifts* ed G K Shenoy and F E Wagner (Amsterdam: North Holland) Ch 6b p 317
[35] Coehoorn R 1990 *Supermagnets, Hard Magnetic Materials* ed G J Long and F Grandjean (Dordrecht: Kluwer) p 133
[36] Khan Y 1973 *Acta Crysallogr.* B **29** 2502